

GRAPHENE WOVEN FABRIC/POLYDIMETHYLSILOXANE COMPOSITES AS FLEXIBLE STRAIN AND TEMPERATURE SENSORS FOR WEARABLE APPLICATIONS

Xu Liu¹, Chen Tang¹, Shuai Xiong¹, Siyuan Xi¹, Xiaohan Du¹, Yuefeng Liu¹, Ying Wu¹, Zhenyu Wang¹, Xi Shen¹, Qingbin Zheng¹, [Jang-Kyo Kim¹](mailto:mejjkim@ust.hk)

¹Department of Mechanical and Aerospace Engineering, The Hong Kong University of Science and Technology, Clear Water Bay, Kowloon, Hong Kong
Email: mejjkim@ust.hk

Keywords: graphene woven fabric, composites, strain sensor, temperature sensor, wearable device

ABSTRACT

Graphene woven fabrics (GWFs) are fabricated by template-directed chemical vapor deposition on Ni templates. Freestanding GWFs with orthogonally interconnected graphene tubes are obtained after etching Ni frameworks. One layer of freestanding GWF is deposited onto a flexible and stretchable polydimethylsiloxane (PDMS) substrate. The change in electrical resistance (ΔR) relative to the original resistance (R_0) is continuously monitored as a function of applied strain while the GWF/PDMS composite is subjected to cyclic uniaxial tension. The normalized resistance of the composite shows a $\sim 670\%$ increase at a tensile strain of 3% and is recovered to zero upon unloading during the loading/unloading cycles, indicating that the composite can be used as flexible strain sensors within the reversible strain range. Besides strain, the composite also shows a normalized resistance change of $\sim 400\%$ with a temperature increase from ambient to 100 °C, confirming a sufficient sensitivity for use as temperature sensors. Such lightweight and highly sensitive, conductive GWF/PDMS composites are excellent candidates as flexible sensors for emerging wearable applications. A wearable musical instrument is demonstrated with integrated GWF/PDMS composites as flexible motion sensor so that one can easily produce music by hand gestures through cellphones.

1 INTRODUCTION

Graphene has attracted significant attention for various sensing applications^{1,2} due to its high electrical conductivity and large specific surface area^{3,4} which facilitate the effective formation of conductive networks. The chemical vapor deposition (CVD) is one of the most promising methods to synthesis continuous graphene structures, which have much fewer defects and impurities, and therefore much higher electrical conductivities than graphene oxide (GO) or reduced GO sheets produced by chemical methods. Moreover, the morphology of the template on which carbon is deposited can be designed so that three-dimensional (3D) interconnected graphene structures, such as graphene foam (GF)⁵ and graphene woven fabric (GWF),⁶ can be produced. These graphene structures are ideal fillers to make composites with homogeneous filler dispersion. The inherently percolated graphene network also enables to achieve very low percolation thresholds of the composites, beneficial to the sensory applications. GF/polydimethylsiloxane (PDMS) composites made by growing graphene on metal foam and coating with PDMS have shown great potential as stretchable strain sensors.^{7,8,9,10} Compared to the cellular GF with irregular graphene networks, GWF has a well-defined interwoven structure with orthogonally interconnected hollow graphene tubes (GTs).¹¹ Such regular conductive network of GWF allows reversible and predictable changes in resistance with strain, making it a more ideal candidate than GF for strain sensor applications. GWF/PDMS composites with a low electrical resistance have shown potential applications in flexible strain sensors^{12,13,14} and touch sensing devices¹⁵. However, few studies have been dedicated to optimizing the CVD process of fabricating GWF for better strain and temperature sensing capabilities. This study is aimed to identify optimized CVD parameters for GWF fabrication and to evaluate the effect of carbon concentration on sensitivity of GWF/PDMS composites to strain and temperature. Freestanding GWFs with orthogonally interconnected GT networks were

fabricated under different carbon concentrations. GWFs were deposited on a flexible PDMS thin film, and the strain and temperature sensing capabilities of GWF/PDMS composites were investigated. Finally, a prototype of wearable musical instrument was developed based on the GWF/PDMS composites to demonstrate their wearable sensing applications.¹⁶ The GWF/PDMS composites were attached to fingers to serve as flexible motion sensor from which music was in real time produced by simple hand gestures through cellphones.

2 EXPERIMENTAL

2.1 GWF synthesis

Ni woven fabric templates were used as substrates for the synthesis of GWFs by template-based CVD method as reported previously.^{11,17,18} The Ni woven fabrics were cleaned with diluted hydrochloride acid (HCl), acetone and deionized (DI) water in sequence by ultrasonication. After drying in an oven for 24 h, the Ni templates were cut into pieces of 10 cm × 5 cm rectangles, which were placed in the quartz tube of the CVD furnace. The furnace was heated from ambient to 1000 °C at a ramp rate of 17 °C/min and the Ni surface was annealed under Ar (200 standard cubic centimeter per minute (sccm)) and H₂ (100 sccm) flows for 1 h. CH₄ was subsequently introduced into the furnace for the deposition of graphene for 20 min. Different CH₄ concentrations, 3 and 10 vol% in Ar and H₂ flows, were used for the parametric study. The furnace was then rapidly cooled to ambient under the same Ar and H₂ flows, and graphene layers were formed on the template surface. Freestanding GWFs were obtained after etching the Ni templates by immersing in a 0.5 M FeCl₃/1 M HCl mixture at 60°C for 2 h.

2.2 Fabrication of GWF/PDMS composites

PDMS solution (Sylgard184, Dow Corning, base agent/curing agent = 10/1 by weight) was stirred for 1 h at room temperature, which was then spin-coated onto the polyethylene terephthalate (PET) thin film at a speed of 200 rpm for 1 min. PDMS thin films were obtained after curing in an oven at 60°C for 20 min. The freestanding GWFs were cut into rectangular shapes (25 × 5 mm) and then deposited onto the pre-cured PDMS thin film with good adhesion between GWF and PDMS. The composites were then cured at 80°C for 2 h and peeled off from PET thin film (Figure 1).

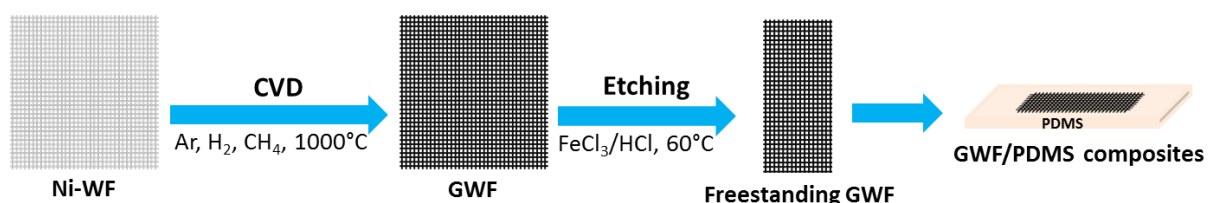


Figure 1. Schematic of the fabrication process of GWF/PDMS composites.

2.3 Characterization

An optical microscope and scanning electron microscopes (SEM) with a 5 kV accelerating voltage were used to characterize the morphologies of freestanding GWFs and composites. The mechanical tests were carried out using a universal testing machine. The tensile samples were loaded with the orientation of GTs aligned along the loading direction at a crosshead speed of 1 mm/min. The cyclic tensile tests were performed for 30 cycles while continuously monitoring the resistance of the composites using a data logger during the tests.

3 RESULTS AND DISCUSSION

3.1 Structures of GWF and GWF/PDMS composites

The freestanding GWFs consisted of interconnected hollow graphene tubes after etching the Ni

templates. The mesh configurations of Ni templates (Figure 2a) were almost entirely retained due to the thick, robust graphene layers grown under the high carbon concentration (i.e., 10 vol%). Good adhesions between GWFs and PDMS were obtained by depositing the freestanding GWF on the partially cured PDMS thin film, so that the GWF was partially embedded in the PDMS matrix after complete curing (Figures 2b and 2c). Such good adhesion could avoid the delamination and thus completely translate the strain from the PDMS matrix to the GWF, which was particularly important for the sensitivity of composites.

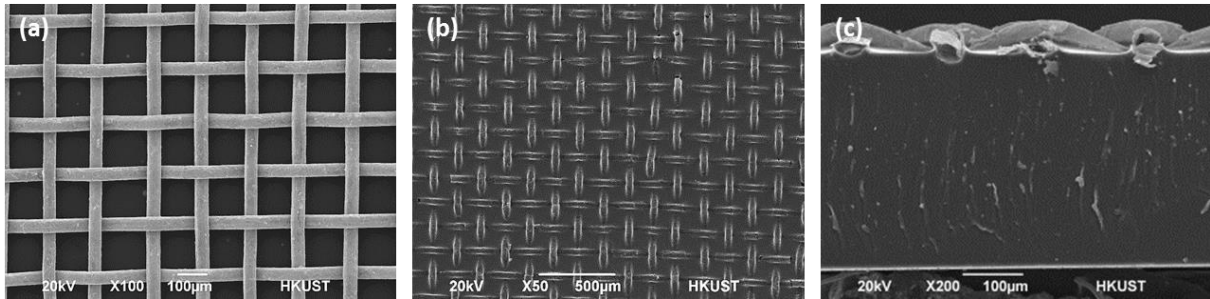


Figure 2. SEM images of (a) freestanding GWF grown from 10 vol% CH₄, (b) the surface view and (c) the cross-sectional view of GWF/PDMS composite.

3.2 Resistance change of GWF/PDMS composites under uniaxial tension

The change in electrical resistance, $\Delta R = R - R_0$, relative to the original resistance, R_0 , was measured as a function of applied strain while the GWF/PDMS composite was subjected to a uniaxial tension, and the results are shown in Figure 3a. Upon tension of the PDMS thin film, the GTs will be subjected to tensile strains, leading to increases in electrical resistance of the composites. The GWF/PDMS composites containing a thicker GWF showed a much higher sensitivity than that with a thinner GWF. The SEM images of the two freestanding GWFs (Figures 3b and 3c) indicate that a higher CH₄ concentration resulted in thicker and more robust GTs. Therefore, the thicker GWFs had more stable and regular mesh configurations once transferred onto the PDMS, while the thinner GWFs tended to shrink upon curing on the PDMS matrix with a wavy structure (Figures 3d and 3e). As a consequence, the composites made from the thicker GWFs presented almost linear increase in resistance with tensile strain, while the composites with the thinner GWFs showed almost no changes in resistance for the initial 0.75% strain because the wavy meshes in the GWFs underwent flattening before effective stretching. In view of the more stable and robust structure with a consistently higher sensitivity to tension, the GWF/PDMS composites containing thicker GWFs grown from 10 vol% CH₄ are considered more suitable for strain sensing applications.

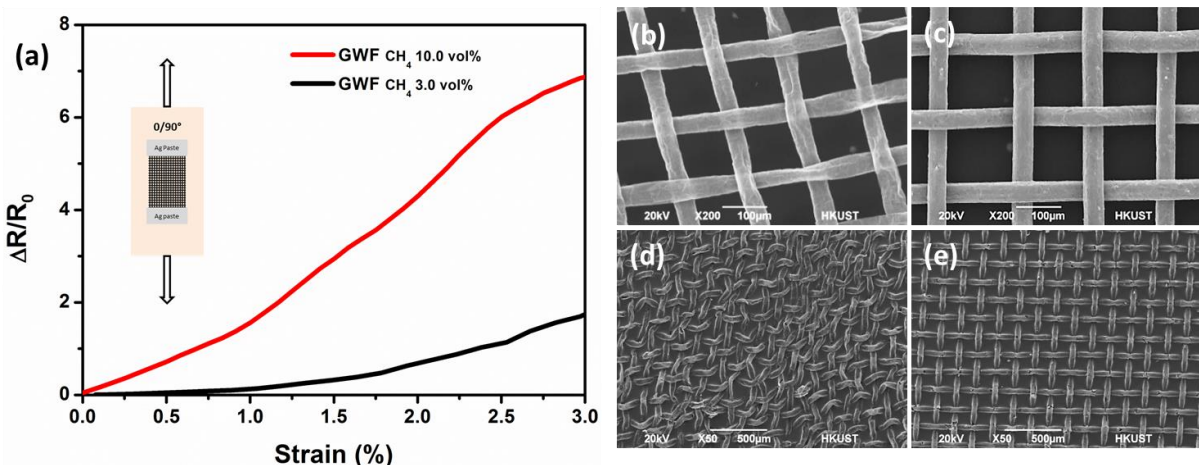


Figure 3. (a) Normalized resistance change ($\Delta R/R_0$) of GWF/PDMS composites as a function of tensile strain. SEM images of freestanding GWFs made from CH₄ concentrations of (b) 3 and (c) 10

vol%; (d) and (e) GWF/PDMS composites made from GWF shown in (b) and (c), respectively.

Figure 4 shows the load and the normalized resistance change of GWF (CH₄ 10.0 vol%)/PDMS composites under cyclic tension to different maximum strains of 1, 2 and 3%. The loads increased linearly to the same peak values for a peak given strain and returned to zero upon unloading during the whole 30 cycles. This observation reflects highly elastic, i.e. reversible, and flexible nature of the GWF/PDMS composites under the given cyclic loading. Similarly, the normalized resistance change increased by ~105, ~340 and ~ 670% upon loading to the said tensile strains, respectively, and the resistance was fully recovered to zero upon unloading. The response was very consistent with almost identical resistance changes during the whole 30 cycles, indicating the reliability of using GWF/PDMS composites as practical strain sensors.

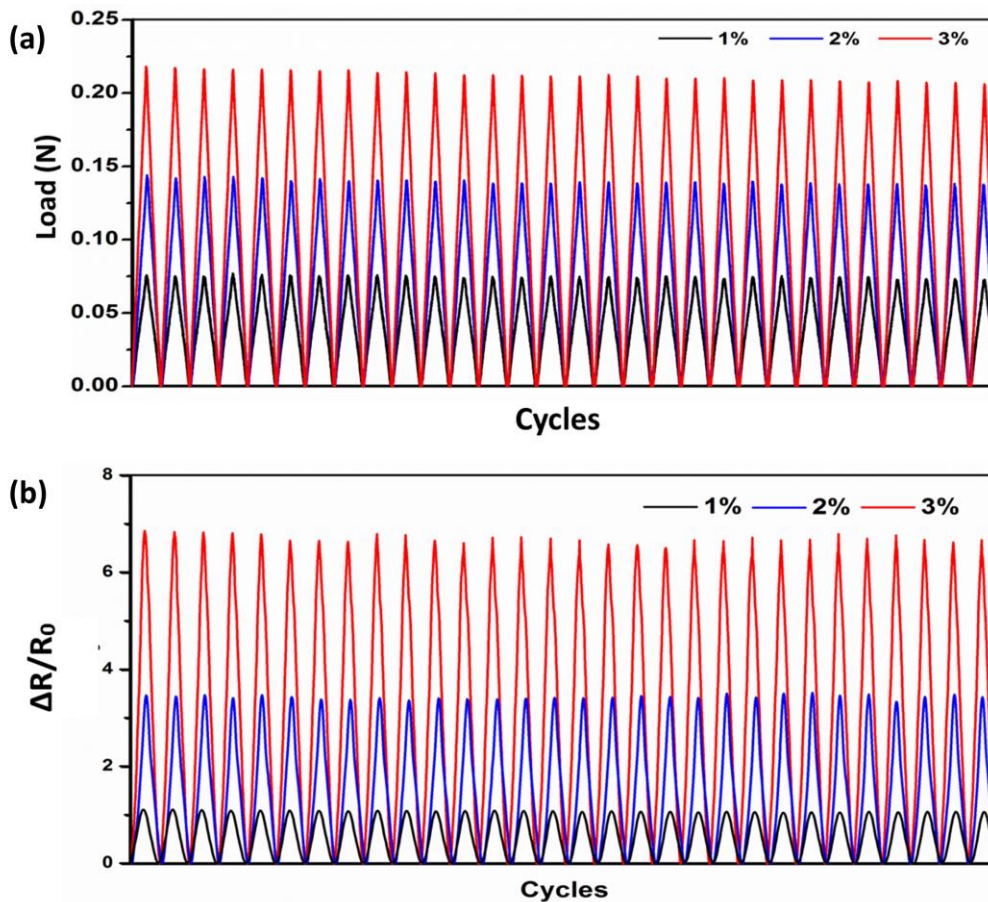


Figure 4. (a) Cyclic tensile loads applied to the GWF/PDMS composites; and (b) the corresponding normalized changes in electrical resistance ($\Delta R/R_0$).

3.3 Resistance change of GWF/PDMS composites with temperature

PDMS is a flexible and transparent polymer with a very high coefficient of thermal expansion (CTE) of $3.0 \times 10^{-4} \text{ }^\circ\text{C}^{-1}$ in the temperature range of $-55 \sim 120 \text{ }^\circ\text{C}$, which can be used as the matrix material for temperature sensing.^{19,20} Figure 5 shows that the normalized resistance change of the GWF/PDMS composites increased with increasing temperature between 0 and 100 $^\circ\text{C}$, which is considered an important temperature range often encountered in our daily life. Similar to the resistance change under uniaxial tension, the composites containing a thicker GWF presented a much higher sensitivity to temperature change than those made from a thinner GWF. The change in resistance of freestanding GWFs without PDMS matrix was also measured. The resistance of GWFs alone showed almost negligible variations with only ~3% fluctuation in the temperature range from 0 to 100 $^\circ\text{C}$. This means

that the resistance change in the GWF/PDMS composites did not arise from the GWF itself because of its very low CTE ($2.0 \times 10^{-6} \text{ }^\circ\text{C}^{-1}$), but arose mostly from the PDMS. When the composites were subjected to heating, the large expansion of PDMS caused the stretching of conductive networks of GTs within the composites, leading to a continuous increase in electrical resistance, depending on the properties of GWFs.

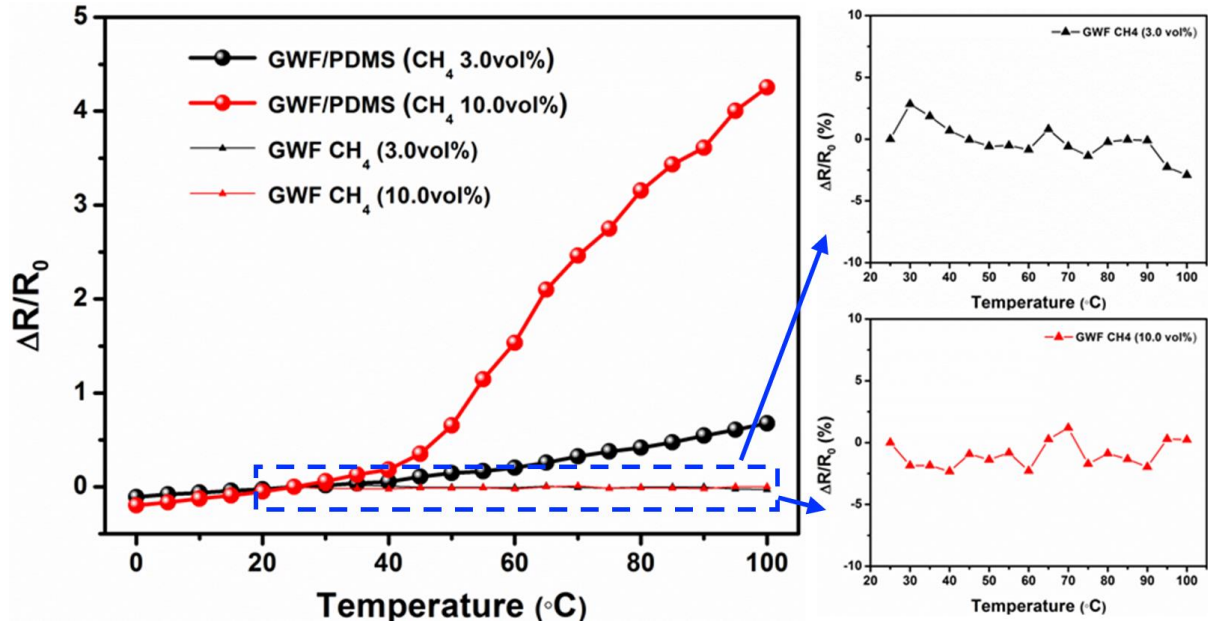
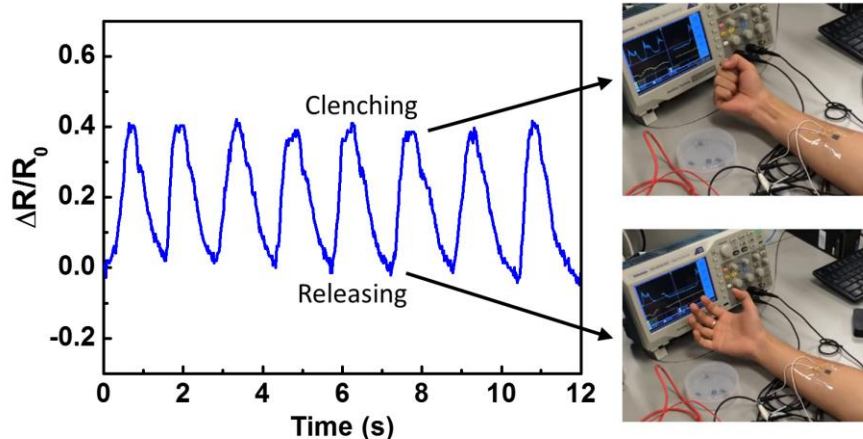


Figure 5. Normalized resistance change ($\Delta R/R_0$) of GWF/PDMS composites during heating. The enlarged views show the small change in resistance of GWF alone with temperature.

3.4 Application of GWF/PDMS composites for wearable musical instruments

The excellent sensitivity of GWF/PDMS composites to strain makes them ideal candidates as flexible sensors for emerging wearable devices. To demonstrate the feasibility of GWF/PDMS composites in sensing motions of body parts, composite sensors were attached to human body parts and the change in resistance due to body motion was measured (Figure 6). One composite sensor was bonded to the forearm with the bandage. An oscilloscope was used to monitor the change in resistance across the sensor simultaneously. The composite sensor was very sensitive to the hand motion, with the increase in resistance by up to 40% when the fist was clenched, and the results were very consistent under the repeated clench and release. This demonstrates the applicability of GWF/PDMS composite sensors in detecting body motions for wearable applications.



Excerpt from ISBN 978-3-00-053387-7

Figure 6. Normalized resistance change of the GWF/PDMS composite sensor attached onto the forearm during cycles of fist clenching and releasing.

The GWF/PDMS composites were further integrated into a wearable musical instrument, which was able to produce music with hand gestures. The resistance changes of flexible sensors made from GWF/PDMS composites due to the bending of fingers were processed and translated into music notes in real time. The whole hardware system consisted of several parts (Figure 7a), including (i) wearable sensors made from GWF/PDMS composites, (ii) an extension board, (iii) a main board (Bluno Beetle), (iv) a wristband that accommodates the extension board, main board and batteries, and (v) the cellphone with software that can generate music notes of different instruments. To ensure good attachment of sensors to the skin, a H-shape sensor with buckles at two ends were fabricated. Such a sensor could be easily wrapped around fingers and taken off. The sensors were connected to the custom-made extension board, which transmitted the resistance changes from the sensors to the main board. The extension board was designed to accommodate up to six sensors with six adjustable resistors to tune the sensitivity of each sensor. The main board was the Bluno Beetle, a developing board that combines the basic Arduino controller and the Bluetooth 4.0 module. The Bluetooth module is capable of wireless communication with the cellphone with a maximum transmission distance as far as 50 m. The extension board and the main board were integrated together with coin cell batteries into a wristband fabricated by 3D printing. The final prototype of the wearable instrument is shown in Figure 7b. Three sensors worn on three fingers were connected to the extension board inside the wristband. An android application was developed to demonstrate the functionality of the wearable instruments (Figure 7c, scan the QR code for demonstrations). The composite sensors on the musician's fingers acted as a remote controller of the music playing from the cellphone. Each sensor controlled one pre-recorded music piece from different instruments, e.g. piano, drum, guitar, etc. The bending of fingers changed the resistance of composite sensors, which triggered the playing of music (Figure 7d).

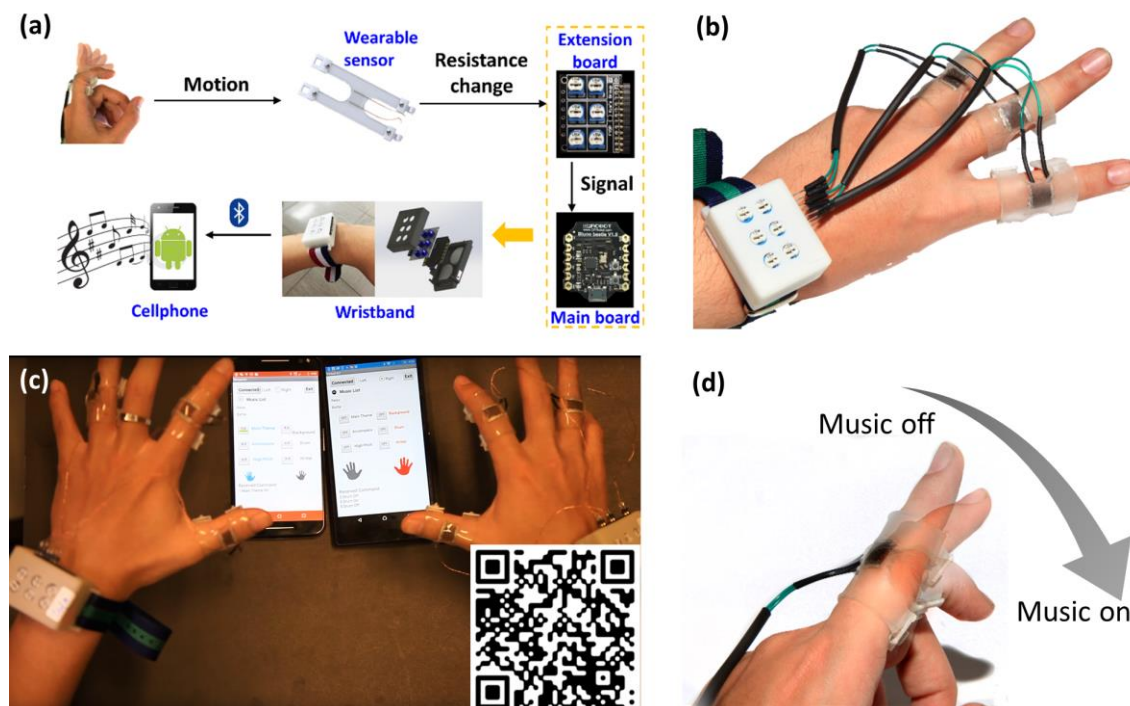


Figure 7. (a) Schematic of the whole wearable musical instrument system; (b) photograph of the prototype of the wearable instrument; (c) demonstration of the use of wearable musical instrument for playing music from cellphones. Scan the QR code for demonstrations; and (d) schematic of manipulating music with finger gestures.

4 CONCLUSION

The present study reports the fabrication of freestanding GWFs by a template-directed CVD method and GWF/PDMS composites. The GWFs consisted of highly conductive GTs interwoven in a well-defined interconnected mesh architecture. The GWF functioned as the electrically conductive network within the composites to sense the external strains and temperature, and thus to present the resistance change as the output.

The flexible GWF/PDMS composites showed high sensitivity and reversibility to uniaxial tension, and the sensitivity depended on the quality of GWFs. The GWF/PDMS composites containing GWF grown from a higher CH₄ concentration of 10 vol% presented a higher sensitivity than that made from a lower concentration of 3 vol%. A high carbon concentration resulted in thicker graphene layers and strong GTs, improving the stability of mesh configuration of GWFs on PDMS. The normalized resistance changes of composites increased by ~105, ~340 and ~670% upon application of tensile strains of 1, 2 and 3%, respectively. These resistances were fully recovered to zero upon unloading during the whole 30 loading/unloading cycles, indicating that the GWF/PDMS composites can be used as flexible strain sensors within the applied reversible strain range. Apart from strains, the GWF/PDMS composites also showed interesting temperature-dependent resistance change. A ~400% increment in normalized electrical resistance was observed when the temperature was increased from ambient to 100°C, confirming a sufficient sensitivity for use as temperature sensors. The practical application of the composites as wearable devices was demonstrated by integrating GWF/PDMS composites into a wearable musical instrument. The transparent and flexible GWF/PDMS composites acted as flexible body motion sensors which sensed and translated the motion of fingers into pre-recorded music via wireless communication devices including a Bluetooth module and cellphones.

ACKNOWLEDGEMENTS

This project was financially supported by the Research Grants Council of Hong Kong SAR (Project Codes: 61203415, 12168119). The authors also appreciate the technical assistance from the Materials Characterization and Preparation Facilities (MCPF) of HKUST.

REFERENCES

1. Samad, Y. A.; Li, Y.; Alhassan, S. M.; Liao, K., Novel graphene foam composite with adjustable sensitivity for sensor applications. *ACS applied materials & interfaces* **2015**, *7* (17), 9195-202.
2. Yuan, W.; Shi, G., Graphene-based gas sensors. *Journal of Materials Chemistry A* **2013**, *1* (35), 10078.
3. Yousefi, N.; Gudarzi, M. M.; Zheng, Q.; Lin, X.; Shen, X.; Sharif, F.; Kim, J. K. Highly self-aligned, ultralarge-size graphene oxide/polyurethane nanocomposites: mechanical properties and moisture permeability. *Composites Part A* **2014**, *49*, 42-50.
4. Yousefi, N.; Sun, X.; Lin, X.; Shen, X.; Jia, J.; Zhang, B.; Tang, B. Z.; Chan, M.; Kim, J. K. Highly aligned graphene/polymer nanocomposites with excellent dielectric properties for high performance electromagnetic interference shielding. *Advanced Materials* **2014**, *26*, 5480-7.
5. Chen, Z.; Ren, W.; Gao, L.; Liu, B.; Pei, S.; Cheng, H. M., Three-dimensional flexible and conductive interconnected graphene networks grown by chemical vapour deposition. *Nature materials* **2011**, *10* (6), 424-8.
6. Li, X.; Sun, P.; Fan, L.; Zhu, M.; Wang, K.; Zhong, M.; Wei, J.; Wu, D.; Cheng, Y.; Zhu, H., Multifunctional graphene woven fabrics. *Scientific reports* **2012**, *2*, 395.
7. Dong, X.; Wang, X.; Wang, L.; Song, H.; Zhang, H.; Huang, W.; Chen, P., 3D graphene foam as a monolithic and macroporous carbon electrode for electrochemical sensing. *ACS applied materials & interfaces* **2012**, *4* (6), 3129-33.
8. Xu, R.; Lu, Y.; Jiang, C.; Chen, J.; Mao, P.; Gao, G.; Zhang, L.; Wu, S., Facile fabrication of three-dimensional graphene foam/poly(dimethylsiloxane) composites and their potential application as strain sensor. *ACS applied materials & interfaces* **2014**, *6* (16), 13455-60.
9. Jeong, Y. R.; Park, H.; Jin, S. W.; Hong, S. Y.; Lee, S.-S.; Ha, J. S., Highly Stretchable and Sensitive Strain Sensors Using Fragmentized Graphene Foam. *Advanced Functional Materials* **2015**, *25* (27), 4228-4236.
10. Chen, M.; Duan, S.; Zhang, L.; Wang, Z.; Li, C., Three-dimensional porous stretchable and conductive polymer composites based on graphene networks grown by chemical vapour deposition and PEDOT:PSS coating. *Chemical communications* **2015**, *51* (15), 3169-72.

11. Liu, X.; Sun, X.; Wang, Z.; Shen, X.; Wu, Y.; Kim, J. K., Planar Porous Graphene Woven Fabric/Epoxy Composites with Exceptional Electrical, Mechanical Properties, and Fracture Toughness. *ACS applied materials & interfaces* **2015**, 7 (38), 21455-64.
12. Li, X.; Zhang, R.; Yu, W.; Wang, K.; Wei, J.; Wu, D.; Cao, A.; Li, Z.; Cheng, Y.; Zheng, Q.; Ruoff, R. S.; Zhu, H., Stretchable and highly sensitive graphene-on-polymer strain sensors. *Scientific reports* **2012**, 2, 870.
13. Yang, T.; Wang, Y.; Li, X.; Zhang, Y.; Li, X.; Wang, K.; Wu, D.; Jin, H.; Li, Z.; Zhu, H., Torsion sensors of high sensitivity and wide dynamic range based on a graphene woven structure. *Nanoscale* **2014**, 6 (21), 13053-9.
14. Yang, T.; Wang, W.; Zhang, H.; Li, X.; Shi, J.; He, Y.; Zheng, Q.-s.; Li, Z.; Zhu, H., Tactile Sensing System Based on Arrays of Graphene Woven Microfabrics Electromechanical Behavior and Electronic Skin Application. *ACS nano* **2015**, 9 (11), 10867–10875.
15. Lee, X.; Yang, T.; Li, X.; Zhang, R.; Zhu, M.; Zhang, H.; Xie, D.; Wei, J.; Zhong, M.; Wang, K.; Wu, D.; Li, Z.; Zhu, H., Flexible graphene woven fabrics for touch sensing. *Applied Physics Letters* **2013**, 102 (16), 163117.
16. Amjadi, M.; Kyung, K.-U.; Park, I.; Sitti, M., Stretchable, Skin-Mountable, and Wearable Strain Sensors and Their Potential Applications: A Review. *Advanced Functional Materials* **2016**, 26 (11), 1678-1698.
17. Jia, J.; Sun, X.; Lin, X.; Shen, X.; Mai, Y. W.; Kim, J. K., Exceptional electrical conductivity and fracture resistance of 3D interconnected graphene foam/epoxy composites. *ACS nano* **2014**, 8 (6), 5774-83.
18. Sun, X.; Liu, X.; Shen, X.; Wu, Y.; Wang, Z.; Kim, J. K., Graphene foam/carbon nanotube/poly(dimethyl siloxane) composites for exceptional microwave shielding. *Composites Part A* **2016**, 85, 199-206.
19. Bowden, N.; Brittain, S.; Evans, A. G.; Hutchinson, J. W.; Whitesides, G. M., Spontaneous formation of ordered structures in thin films of metals supported on an elastomeric polymer. *Nature* **1998**, 393 (6681), 146-149.
20. Chiche, A.; Stafford, C. M.; Cabral, J. T., Complex micropatterning of periodic structures on elastomeric surfaces. *Soft Matter* **2008**, 4 (12), 2360-2364.